

Electronic Supplementary Information

Two-terminal DSSC/Silicon Tandem Solar Cells exceeding 18%-Efficiency.

Jeong Kwon,^{‡a} Min Ji Im,^{‡b,c} Chan Ul Kim,^{b,c} Sang Hyuk Won,^b Sung Bum Kang,^b Sung Ho Kang,^d In Taek Choi,^d

Hwan Kyu Kim,^d In Ho Kim,^e Jong Hyeok Park,^{f*} and Kyoung Jin Choi^{b,c*}

^aDepartment of Chemical Engineering, Sungkyunkwan University, Suwon 16419, South Korea.

^bSchool of Materials Science and Engineering, Ulsan National Institute of Science and Technology (UNIST), Ulsan 44919, South Korea

^cKIST-UNIST Ulsan Center for Convergent Materials (KUUC), Ulsan 44919, South Korea

^dDepartment of Advanced Materials Chemistry, Korea University, Sejong-ro, Sejong 30019, South Korea

^eElectronic Materials Research Center, Korea Institute of Science and Technology, Hwarangno 14 gil-5, Seongbuk-gu, Seoul 02792, South Korea

^fDepartment of Chemical and Biomolecular Engineering, Yonsei University, 50 Yonsei-ro, Seodaemun-gu, Seoul 03722, South Korea

*Corresponding authors

E-mail address: lutts@yonsei.ac.kr, choi@unist.ac.kr

Characterizations

Fig. S1. The DSSC performances as a function of TiO₂ film thickness.

Fig. S2. The performances of the bottom c-Si devices filtered by the top DSSC.

Fig. S3. (a) Nyquist plots, (b) Tafel-polarization curves of different thickness of PEDOT dummy cells, (c) Transmittance and (d) photo images of the different thickness of PEDOT on glass substrates.

Fig. S4. The morphologies of PEDOT:FTS layers depending on the amount of retardant.

Fig. S5. J_{sc} , V_{oc} , FF and PCE of DSSC with Pt and PEDOT:FTS CEs. Error bars represents minimum and maximum values, and the middle line in each box represents the median value. Upper and lower error bars in the box represent the third quartile (Q3) and first quartile (Q1), respectively, and box thickness represents interquartile Q3–Q1. Squares indicate mean values

Fig. S6. J-V curve of tandem solar cell with Pt interlayer.

Fig. S7. PCE histograms of 65 devices for the internal tandem solar cells

Fig. S8. The energy level diagram of the 2-terminal tandem solar cell.

Fig. S9. Fabrication process of DSSC/Si tandem solar cell.

Table S1. Current-voltage characteristics of DSSCs depend on the TiO₂ thickness.

Table S2. Current-voltage characteristics of bottom c-Si devices filtered by the top DSSC.

Table S3. Current-voltage characteristics of tandem solar cell with Pt interlayer.

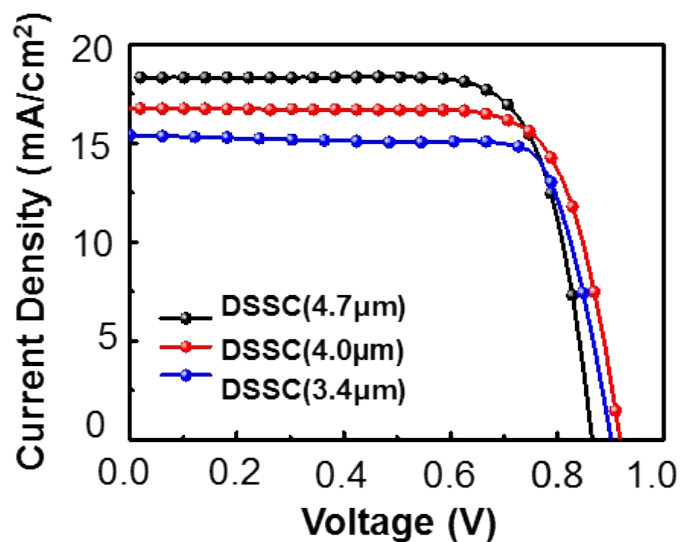


Fig. S1. The DSSC performances as a function of TiO₂ film thickness.

Table S1. Current-voltage characteristics of DSSCs depending on the TiO₂ thickness.

Devices	J _{sc} (mA/cm ²)	V _{oc} (V)	FF (%)	Efficiency (%)
DSSC (4.7 μm)	18.3	0.864	75.7	12.0
DSSC (4.0 μm)	16.8	0.907	75.7	11.4
DSSC (3.4 μm)	15.4	0.900	78.8	11.0

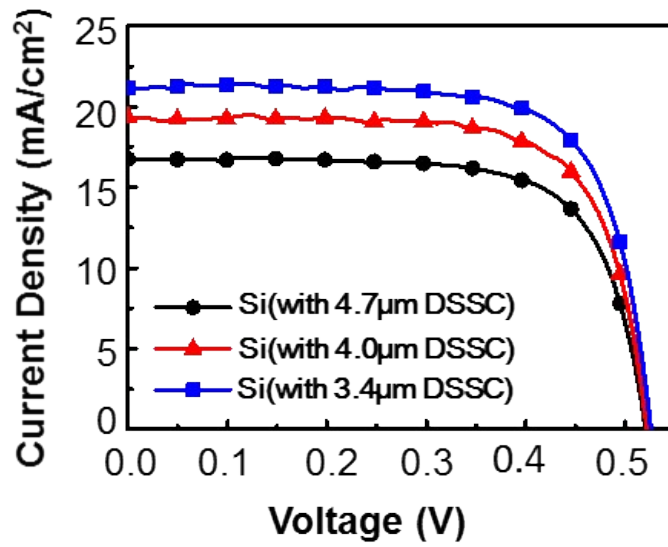


Fig. S2. The performances of the bottom c-Si devices filtered by the top DSSC.

Table S2. Current-voltage characteristics of bottom c-Si devices filtered by the top DSSC.

Devices	J_{sc} (mA/cm ²)	V_{oc} (V)	FF (%)	Efficiency (%)
Si (with 4.7 μm DSSC)	16.7	0.521	71.5	6.23
Si (with 4.0 μm DSSC)	19.2	0.522	71.9	7.23
Si (with 3.4 μm DSSC)	21.2	0.526	72.6	8.09

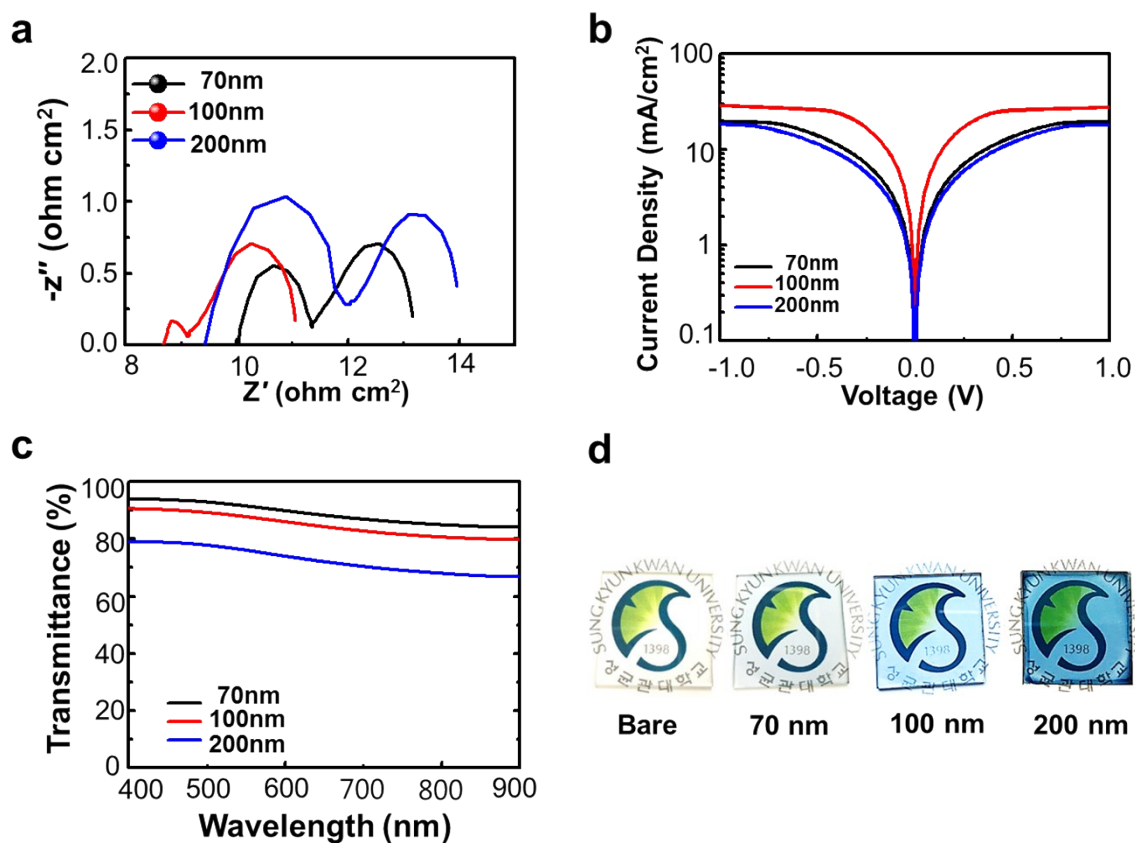


Fig. S3. (a) Nyquist plots, (b) Tafel-polarization curves of different thickness of PEDOT dummy cells, (c) Transmittance and (d) photo images of the different thickness of PEDOT on glass substrates.

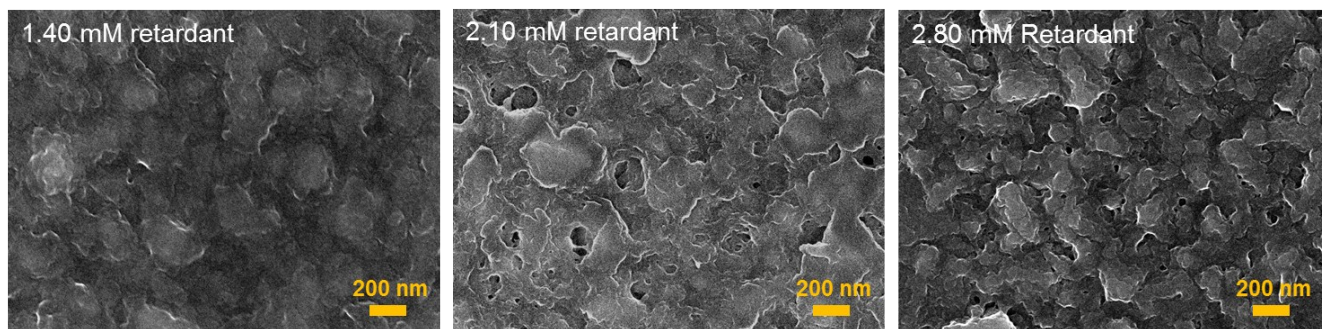


Fig. S4. The morphologies of PEDOT:FTS layers depending on the amount of retardant.

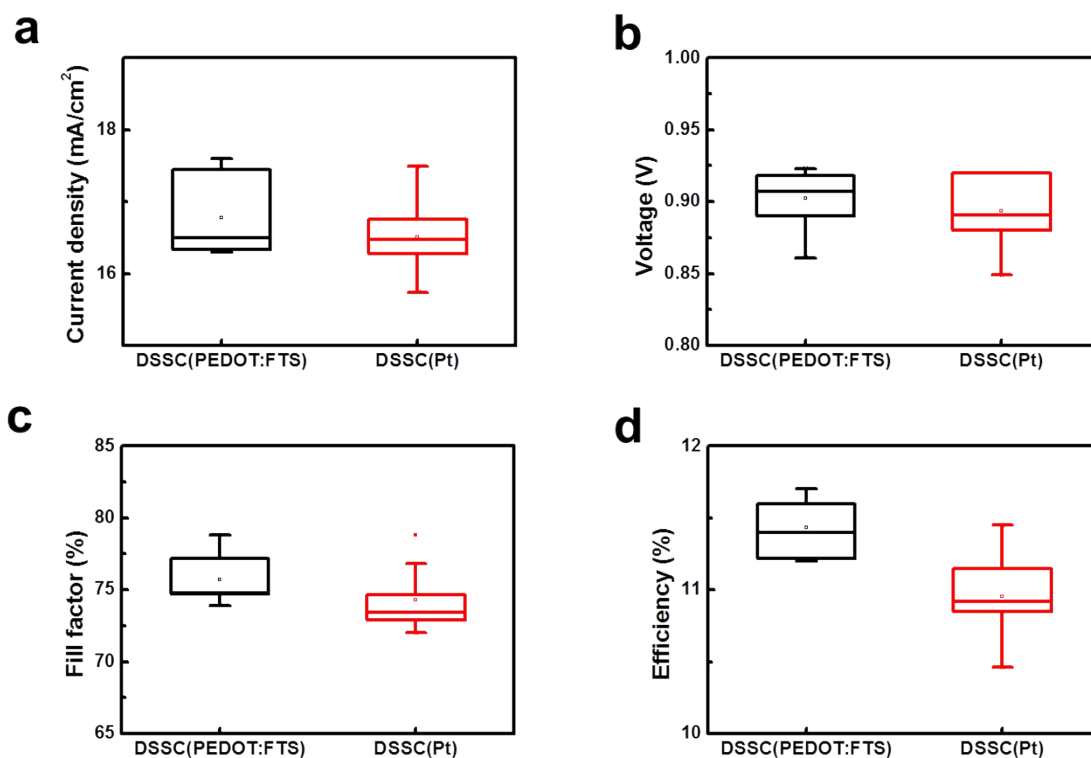


Fig. S5. J_{sc} , V_{oc} , FF and PCE of DSSC with Pt and PEDOT:FTS CEs. Error bars represents minimum and maximum values, and the middle line in each box represents the median value. Upper and lower error bars in the box represent the third quartile (Q3) and first quartile (Q1), respectively, and box thickness represents interquartile Q3–Q1. Squares indicate mean values

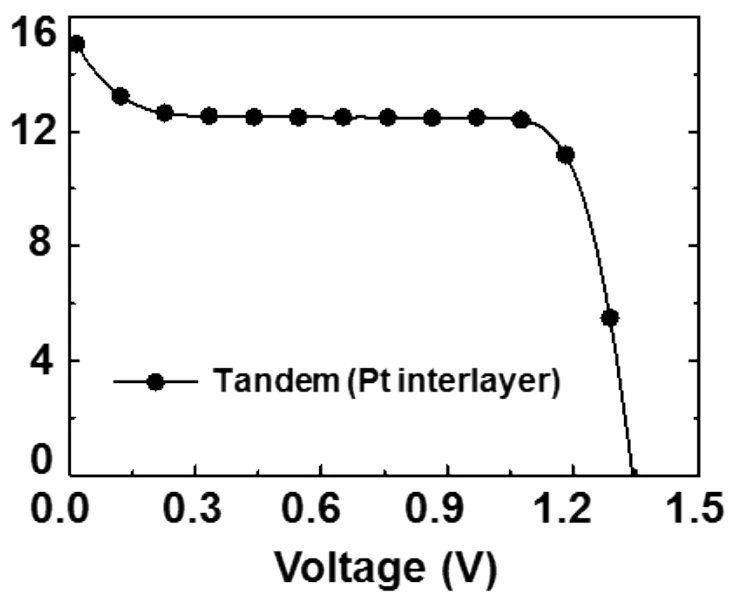


Fig. S6. J-V curve of tandem solar cell with Pt interlayer.

Table S3. Current-voltage characteristics of tandem solar cell with Pt interlayer.

Jsc (mA/cm²)	Voc (V)	FF (%)	Efficiency (%)
15.21	1.34	66.95	13.67

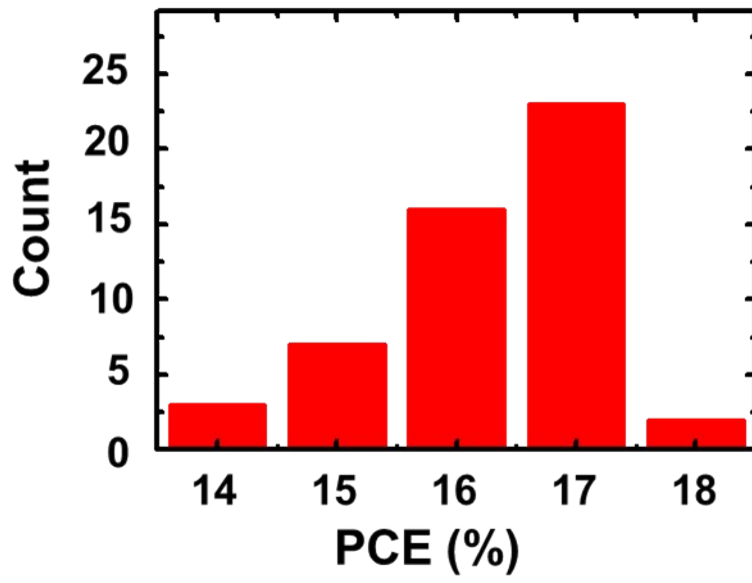


Fig. S7. PCE histograms of 65 devices for the internal tandem solar cells.

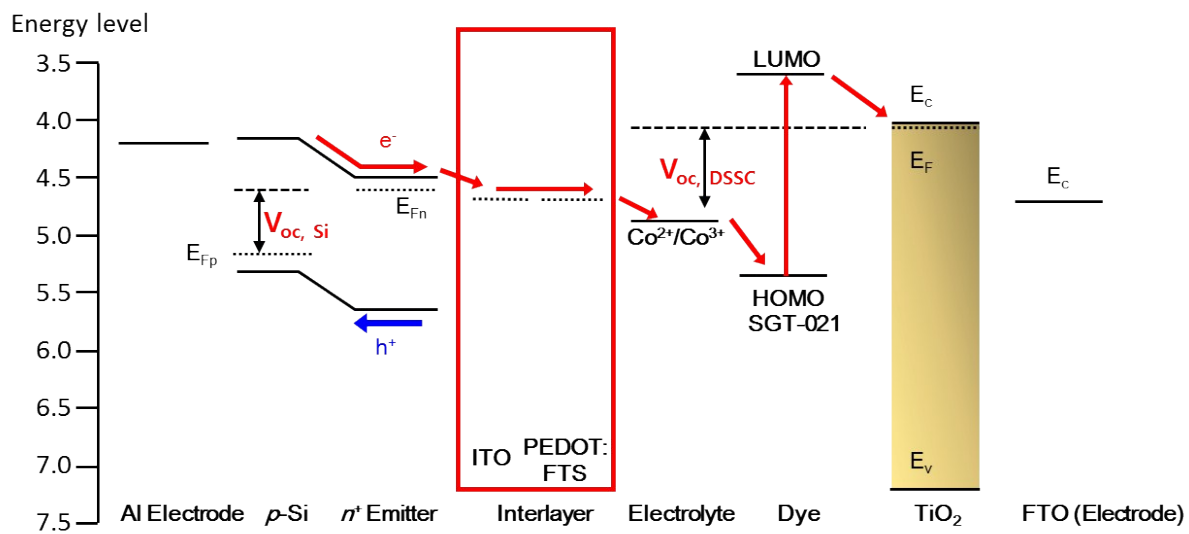


Fig. S8. The energy level diagram of the 2-terminal tandem solar cell.

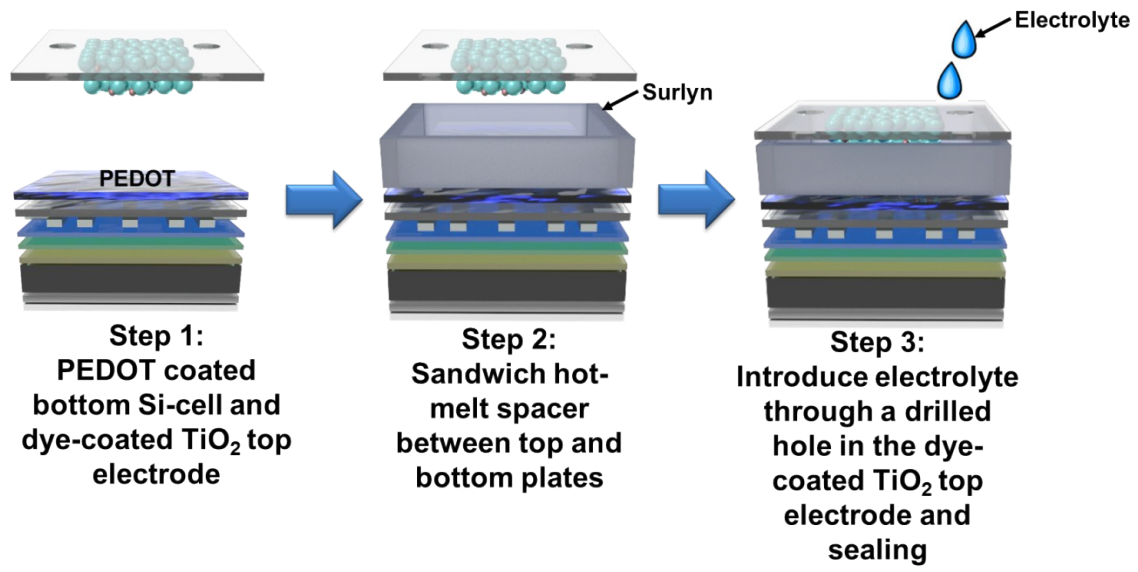


Fig. S9. Fabrication process of DSSC/Si tandem solar cell.